ELSEVIER

www.elsevier.nl/locate/jorganchem

Journal of Organometallic Chemistry 584 (1999) 48–57

Journal of Organometallic Chemistry

Synthesis, structural characterization and solvatochromic studies of a series of Schiff base-containing triosmium alkylidyne carbonyl clusters

Wai-Yeung Wong [a,*], Wing-Tak Wong [b]

[a] *Department of Chemistry, Hong Kong Baptist University, Waterloo Road, Kowloon Tong, Hong Kong*
[b] *Department of Chemistry, The University of Hong Kong, Pokfulam Road, Hong Kong, Hong Kong*

Received 12 December 1998

Abstract

A series of new Schiff base-containing triosmium alkylidyne carbonyl clusters $[Os_3(\mu\text{-}H)_2(CO)_9(\mu_3\text{-}CNC_5H_4CH{=}NC_6H_4R)]$ (R = H, NMe_2, SMe, CMe_3, NH_2, Br, Cl, OC_nH_{2n+1}, $n = 1$, 6, 7 or 9) have been prepared by reaction of $[Os_3(\mu\text{-}H)_3(CO)_9(\mu_3\text{-}CCl)]$ with one equivalent of 1,8-diazabicyclo[5.4.0]undec-7-ene in the presence of a ten-fold excess of the Schiff base ligands $NC_5H_4CH{=}NC_6H_4R$ at room temperature. Analogous triosmium carbonyl clusters bearing 4′-methoxy-4-stilbazole or 4-(4-nitrobenzyl)pyridine moiety at the apical carbon centre have also been synthesized using a similar deprotonation method. The molecular structures of selected complexes have been established by X-ray crystallography. UV–vis spectroscopy suggests that this class of compounds displays significant negative solvatochromic effect in an organic medium.

Keywords: Osmium; Alkylidyne; Clusters; Solvatochromism; Crystal structures

1. Introduction

Transition-metal complexes with such ligands as 4′-alkoxy-4-stilbazoles ($NC_5H_4CH{=}CHC_6H_4OR$) and 4-pyridylmethylene-4′-alkoxyanilines ($NC_5H_4CH{=}NC_6H_4OR$) represent an active area of research in view of their interesting optical, photophysical and liquid-crystalline properties. However, few solid-state structures of these complexes have been reported [1].

As a continuation of a broad study of the chemistry and properties of trinuclear alkylidyne carbonyl clusters of the type $[M_3(\mu\text{-}H)_2(CO)_9(\mu_3\text{-}CY)]$ (M = Ru, Os; Y = Lewis bases) [2], we report in this article on the preparation of a series of triosmium carbonyl clusters $[Os_3(\mu\text{-}H)_2(CO)_9(\mu_3\text{-}CNC_5H_4CH{=}NC_6H_4R)]$ (R = H, NMe_2, SMe, CMe_3, NH_2, Br, Cl, OC_nH_{2n+1}, $n = 1$, 6, 7 or 9), containing pyridyl Schiff base ligands (**I**) as well as two similar complexes with 4′-methoxy-4-stilbazole (**II**) or 4-(4-nitrobenzyl)pyridine (**III**) as the ligands.

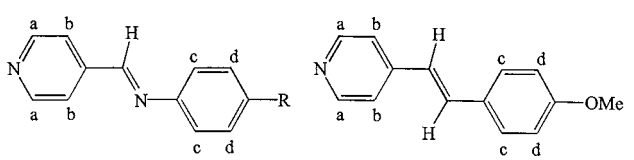

I **II**

R = H, NMe_2, SMe, CMe_3, NH_2, Br, Cl, OC_nH_{2n+1}, n = 1, 6, 7 or 9

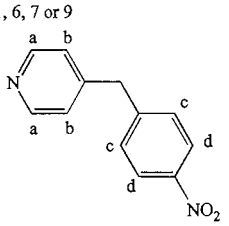

III

This class of trinuclear alkylidyne clusters has been shown to adopt a zwitterionic formulation and display strong negative solvatochromism [1e,f,3]. A program was thus initiated to study the influence of different substituents attached to the ligands with varying electronic properties on the overall characteristics of the system. All these new compounds have been fully characterized by IR, NMR and UV–vis spectroscopies and

* Corresponding author. Fax: +852-2339-7348.
E-mail address: rwywong@net1.hkbu.edu.hk (W.-Y. Wong)

0022-328X/99/$ - see front matter
PII: S0022-328X(99)00091-1

by FAB mass spectrometry. The molecular structures of four of them have been established by single-crystal X-ray analyses.

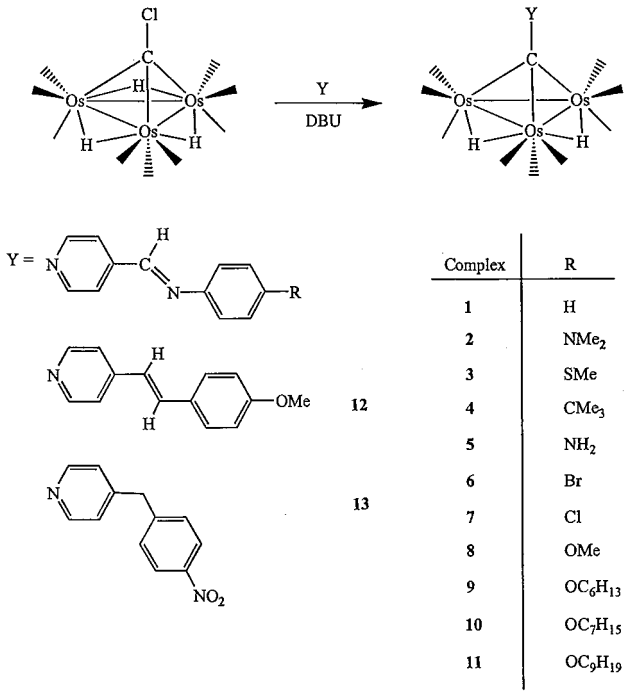

Complex	R
1	H
2	NMe_2
3	SMe
4	CMe_3
5	NH_2
6	Br
7	Cl
8	OMe
9	OC_6H_{13}
10	OC_7H_{15}
11	OC_9H_{19}

Scheme 1.

Table 1
IR and FAB MS data for complexes **1–13**

Complex	IR (ν_{CO} (cm^{-1}), CH_2Cl_2)	FAB MS (m/z)	
		Experimental	Simulated
1	2090m, 2055vs, 2025vs, 1984s, 1952m, 1936m	1020	1020
2	2089m, 2054vs, 2023vs, 1982s, 1950m, 1935m	1063	1063
3	2090m, 2055vs, 2024vs, 1983s, 1950m, 1936m	1066	1066
4	2090m, 2055vs, 2024vs, 1983s, 1951m, 1936m	1076	1076
5	2090m, 2055vs, 2024vs, 1983s, 1951m, 1935m	1035	1035
6	2090m, 2055vs, 2025vs, 1984s, 1951m, 1936m	1098	1098
7	2090m, 2055vs, 2025vs, 1984s, 1952m, 1936m	1054	1054
8	2090m, 2055vs, 2024vs, 1983s, 1951m, 1936m	1050	1050
9	2090m, 2055vs, 2024vs, 1983s, 1951m, 1935m	1120	1120
10	2089m, 2055vs, 2024vs, 1982s, 1951m, 1935m	1134	1134
11	2090m, 2055vs, 2024vs, 1983s, 1950m, 1935m	1162	1162
12	2088m, 2053vs, 2022vs, 1981s, 1949m, 1932m	1049	1049
13	2089m, 2055vs, 2024vs, 1984s, 1951m, 1935m	1052	1052

2. Results and discussion

2.1. Syntheses

All the Schiff base ligands $NC_5H_4CH{=}NC_6H_4R$ are prepared in good yields by the condensation of 4-pyridinecarboxaldehyde and the corresponding substituted aromatic amines [4]. The *trans*-stilbazole is obtained in a reasonable yield by the Wittig reaction of 4-pyridinecarboxaldehyde with 4-methoxybenzyltriphenylphosphonium chloride [5]. Triosmium alkylidyne carbonyl clusters of the type $[Os_3(\mu\text{-}H)_2(CO)_9(\mu_3\text{-}CY)]$ (Y = Schiff bases **1–11**, 4′-methoxy-4-stilbazole **12** and 4-(4-nitrobenzyl)pyridine **13**) are prepared from $[Os_3(\mu\text{-}H)_3(CO)_9(\mu_3\text{-}CCl)]$ and the corresponding ligands according to the DBU-initiated deprotonation method (Scheme 1) [6]. All clusters are isolated by preparative TLC on silica and purified by recrystallization. Complexes **1–11** are all deeply coloured reddish brown solids, whereas complexes **12** and **13** are isolated as bright red and orange crystalline solids, respectively.

2.2. Solution spectroscopy

The formulae of all the new complexes were first established by FAB MS, IR and ^{1}H-NMR spectroscopies. Table 1 summarizes the IR and MS spectral data for those complexes. Their IR spectra in dichloromethane have an almost identical ν_{CO} band pattern in the region 2200–1600 cm^{-1} and are reminiscent of other triosmium alkylidyne clusters with a similar formulation [3]. This indicates that the pyridyl moiety coordinates to the μ_3-carbon atom in an upright manner without affecting the symmetry of each molecule. Complexes **1–13** all show molecular ion envelopes of high to medium intensity in the positive FAB mass spectra, conforming to the stoichiometry of each compound. Sequential loss of carbonyl ligands is also observed.

The ^{1}H-NMR spectra of all the complexes show resonances expected for the ligands Y and the two bridging Os–H hydrides on the cluster framework (Table 2). The downfield displacement of the proton NMR signals associated with the coordinated ligands in **1–13**, as compared to those resonances for the corresponding free ligands, suggests that the pyridyl nitrogen is bonded to the electron-withdrawing Os_3C core. Such shifts can be as large as ca. 1.0 ppm for the proton H_a in most cases. For each complex, both the NC_5H_4 and C_6H_4 rings are analyzed as AA′BB′ spin systems, with two pairs of pseudo doublets of roughly equal intensities shown in the ^{1}H-NMR spectra. As revealed by the

Table 2
^{1}H-NMR chemical shifts (ppm) and coupling constants (Hz) for complexes **1**–**13** in CD_2Cl_2

Complex	H_a	H_b	–CH=N–	H_c	H_d	Other signals	OsH
1	9.73	7.88	8.57(s)	←———	7.43 (m, C_6H_5)	———→	−18.83(s)
2	9.58 J_{ab} 7.0	7.80	8.56(s)	7.47 J_{cd} 8.8	6.75	3.04 (s, NMe_2)	−18.88(s)
3	9.70 J_{ab} 7.0	7.86	8.60(s)	7.37 J_{cd} 8.9	7.33	2.53 (s, SMe)	−18.83(s)
4	9.71 J_{ab} 7.0	7.88	8.60(s)	7.49 J_{cd} 8.7	7.35	1.35 (s, CMe_3)	−18.84(s)
5	9.62 J_{ab} 7.1	7.82	8.56(s)	7.37 J_{cd} 8.8	6.73	4.07 (br, NH_2)	−18.88(s)
6	9.73 J_{ab} 7.1	7.87	8.55(s)	7.60 J_{cd} 8.8	7.27	–	−18.81(s)
7	9.73 J_{ab} 7.0	7.87	8.55(s)	7.44 J_{cd} 8.9	7.34	–	−18.81(s)
12 [a]	9.42 J_{ab} 7.1	7.43	–	7.60(m)	6.96(m)	3.86 (s, OMe)	−18.96(s)
13	9.53 J_{ab} 6.8	8.26	–	7.46 J_{cd} 8.8	7.24	4.07 (s, CH_2)	−19.00(s)

Complex	H_a	H_b	–CH=N–	H_c	H_d	$-OCH_2-$	$-(CH_2)_n-$	$-CH_3$	OsH
8	9.59 J_{ab} 7.0	7.77	8.50(s)	7.37 J_{cd} 9.0	6.90	–	–	3.77(s)	−18.93(s)
9	9.67 J_{ab} 7.1	7.85	8.58(s)	7.44 J_{cd} 9.0	6.97	4.01(t) J 6.6	1.27–1.85	0.92(m)	−18.85(s)
10	9.67 J_{ab} 7.0	7.85	8.58(s)	7.44 J_{cd} 8.9	6.97	4.01(t) J 6.6	1.26–1.83	0.89(m)	−18.85(s)
11	9.67 J_{ab} 6.8	7.85	8.58(s)	7.44 J_{cd} 8.8	6.97	4.01(t) J 6.6	1.12–1.85	0.89(m)	−18.86(s)

[a] The two signals for the CH=CH protons overlap respectively with that of H_c and H_d.

^{1}H-NMR data for the substituents R of the Schiff bases in **1**–**11**, there is virtually no shift in δ values for these substituents between the clusters and the free ligands. In addition to this, the *trans*-stilbazole complex **12** shows a ^{13}C-NMR signal at δ 55.83 for the methoxy group in CD_2Cl_2, which is more or less unchanged compared to the value of δ 55.37 for the free ligand.

2.3. Solvatochromic studies

As an important part of the study on the aforementioned cluster complexes, the electronic absorption spectra of selected complexes in a range of organic solvents with widely different polarities have been measured and the results are presented in Table 3. The lowest energy feature in each of these complexes is extremely solvent dependent and displays significant negative solvatochromism. As previously reported, investigations based on molecular orbital calculations assign this band to the metal-to-ligand charge transfer (MLCT) transition [3a,6a]. On the other hand, the higher energy absorptions are relatively insensitive to changes in solvent. Such an observation strongly conforms to the zwitterionic formulation of these cluster species in their electronic ground state which can be represented by the canonical structures shown in Fig. 1. In fact, they can be considered to contain polarizable donor-π-acceptor structural motif and a less polar excited state is expected upon MLCT excitation. For compounds **8** and **12**, where only a difference in the linking group (CH=N for **8**, CH=CH for **12**) is observed, the electronic absorption spectral data indicate that the low energy MLCT transition for **8** occurs at a lower energy than that of **12**. This is probably due to

Table 3
UV–vis excitation maxima for selected complexes

Compound	λ_{max} (nm) ($\varepsilon \times 10^{-3}$ (dm^3 $mol^{-1}cm^{-1}$))			
	$CH_3(CH_2)_4-CH_3$	CCl_4	CH_2Cl_2	$(CH_3)_2CO$
1	–	626 (8.2)	582 (8.4)	542 (7.1)
2	616 (19.1)	613 (16.9)	585 (23.7)	558 (15.7)
	516 (21.9)	520 (19.5)	514 (19.4)	
3	637 (5.0)	625 (3.3)	584 (5.6)	547 (5.4)
	443 (5.4)	430 (5.1)	443 (6.6)	424 (6.6)
7	–	641 (15.4)	592 (15.2)	547 (14.2)
8	628 (12.7)	620 (11.7)	577 (11.4)	536 (9.6)
			422 (13.0)	413 (11.9)
9	622 (4.3)	614 (3.8)	575 (4.0)	539 (4.0)
	416 (4.8)	417 (4.3)	426 (4.8)	413 (4.9)
12	581 (5.2)	575 (7.7)	534 (6.9)	504 (7.3)

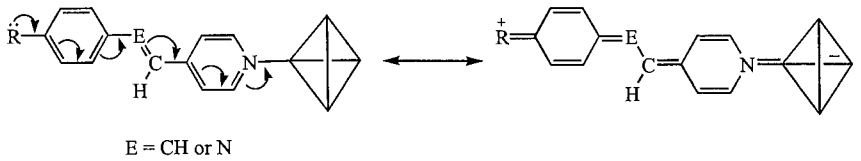

Fig. 1. Zwitterionic formulations of the triosmium alkylidyne carbonyl clusters.

the increasing conjugation effect of the CH=CH group that stabilizes the ground state of the molecule as compared to the CH=N moiety. It is also worth pointing out that the MLCT bands for the alkoxy homologous complexes **8**–**11** all essentially absorb radiation at similar wavelengths in the same solvents, although slight differences in their ε values are apparent.

2.4. Crystal structure analyses

For all complexes **1**–**13** that were fully characterized by spectroscopic methods, the solid-state structures of four of them have been ascertained by X-ray crystallography. Single crystals of **7**, **8**, **12** and **13** suitable for diffraction studies were grown by slow evaporation of their respective solutions in an *n*-hexane/CH_2Cl_2 solvent mixture at room temperature (r.t.). The molecular structures of **7**, **8**, **12** and **13** are depicted in Figs. 2–5, respectively, together with the atom-numbering scheme. Relevant bond distances and angles are listed in Tables 4–7. Each of these structures consist of a triosmium alkylidyne metal core arrangement with the corresponding pyridyl moiety bonded to the μ_3-bridging alkylidyne carbon atom. There are three terminal carbonyl ligands on each vertex. Essentially, the alkylidyne metal cores in these structures show no major variations when compared to those of other substituted pyridine analogues described previously [3a, 6b]. The mean Os–C(alkylidyne) distances range from 2.08(1) to 2.100(7) Å. The two bridging metal hydrides, evident from the ^{1}H-NMR spectra, are located using Orpen's potential energy minimization procedures [7]. The two hydride-bridged Os–Os bonds (mean distance 2.8708(9)–2.8800(5) Å) are significantly longer than the unbridged Os–Os edge (mean distance 2.7579(9)–2.7706(5) Å). This is consistent with the general observation that the metal–metal bond length increases when it is bridged by a hydride atom with the metal hydride relatively in plane with respect to the metal triangle [8]. There are no unusual structural or bonding features in the organic moieties of these complexes. The aromatic rings adopt twisted conformations in the solid states of **7**, **8** and **12**, as revealed from the non-zero dihedral angles between them (5.5, 3.2 and 13.1°, respectively). The phenyl ring in **13**, however, shows considerable twisting at the sp^3 carbon atom C(16), with the angle C(13)–C(16)–C(17) determined to be 114(1)° and a dihedral angle between the pyridyl and the phenyl rings of 86.8°. The nitro group, as in other aromatic organic molecules, is characterized by the delocalization observed along

$$O\cdots N\cdots O$$

accompanied by a slight shortening of the typical N–O bond. In this case, the bonds N(2)–O(10) and N(2)–O(11) are, respectively 1.13(2) and 1.19(2) Å long and the angle O(10)–N(2)–O(11) is 128(3)°.

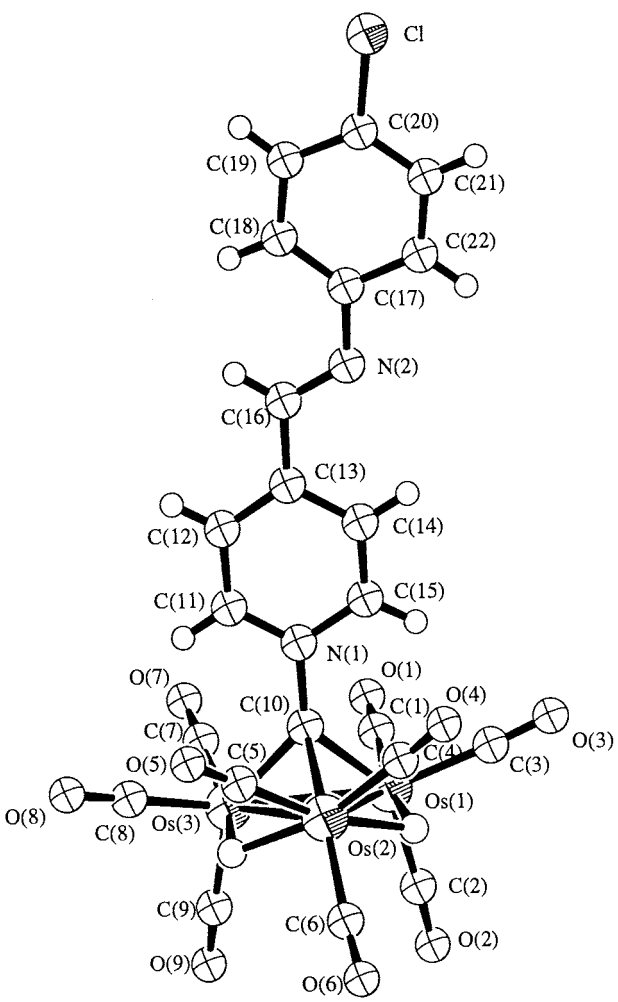

Fig. 2. Molecular structure of $[Os_3(\mu H)_2(CO)_9(\mu_3\text{-}CNC_5H_4CH{=}NC_6H_4Cl)]$ (**7**) showing the atom-numbering scheme.

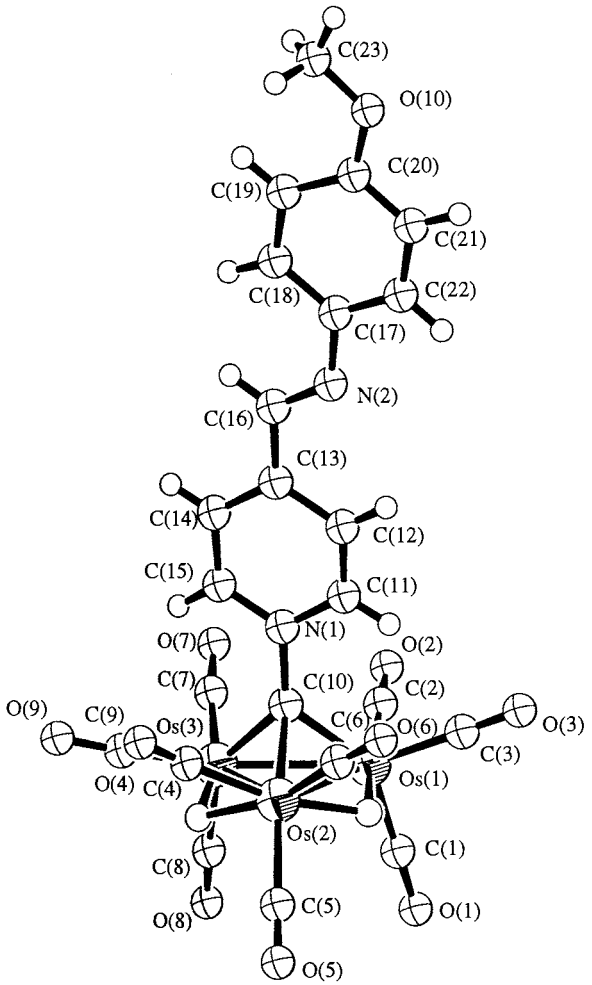

Fig. 3. Molecular structure of $[Os_3(\mu\text{-}H)_2(CO)_9(\mu_3\text{-}CNC_5H_4CH{=}NC_6H_4OMe)]$ (**8**) showing the atom-numbering scheme.

3. Conclusions

A series of polarizable triosmium alkylidyne carbonyl clusters containing 4-pyridylmethylene-4′-alkoxyanilines as ligands have been synthesized and structurally characterized. This family of compounds displays interesting negative solvatochromism and may provide useful information for the study of solvent effects on MLCT bands in transition metal complexes. It is likely that their associated charge separation and solvatochromic properties make them an important candidate in the field of non-linear optics. Our present work has also demonstrated the more effective conjugation through the CH=N bond in the Schiff base-containing cluster than the CH=CH bridge in the stilbazole-substituted complex, which leads to a reduction of the energy band gap between the highest occupied molecular orbitals (HOMO) and the lowest unoccupied molecular orbitals (LUMO).

4. Experimental

4.1. General procedures

None of the compounds reported is particularly air-sensitive, but all manipulations were carried out under an atmosphere of dry dinitrogen. Solvents were predried and distilled from appropriate drying agents [9]. All chemicals, except where stated, were purchased from commercial sources and used as received. The compounds $[Os_3(\mu\text{-}H)_3(CO)_9(\mu_3\text{-}CCl)]$ [10] and $NC_5H_4CH{=}NC_6H_4Br$ [1e] were prepared by literature methods. IR spectra were recorded as CH_2Cl_2 solutions on a Perkin–Elmer 1000 or Bio-Rad FTS-7 IR spectrometer using 0.5 mm solution cells. The ^{1}H-NMR spectra were recorded on a Jeol EX270 FT-NMR spectrometer using deuteriated solvents as lock and the residual protons in the solvent as references. Chemical shifts are reported downfield positive relative to $SiMe_4$. Mass spectra were recorded on a Finnigan MAT 95

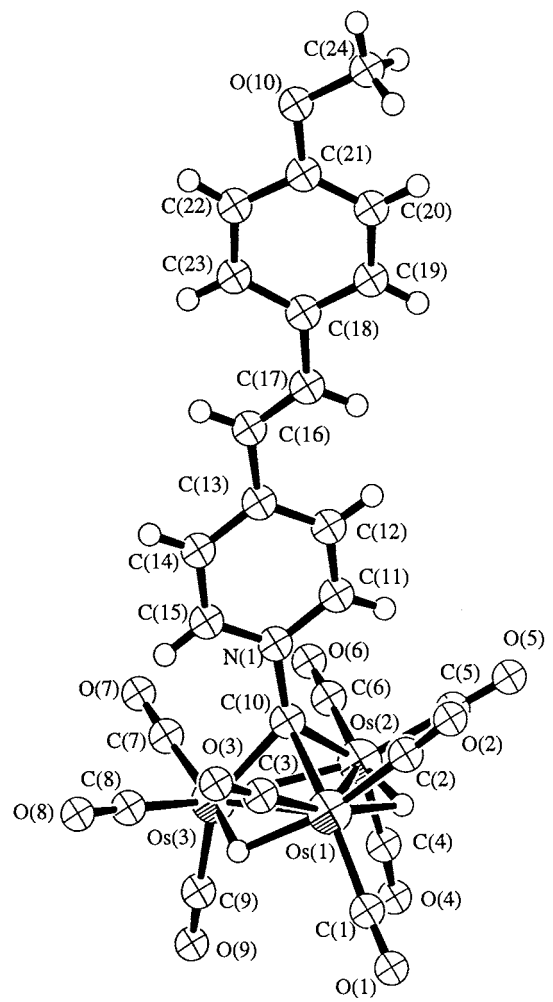

Fig. 4. Molecular structure of $[Os_3(\mu\text{-}H)_2(CO)_9(\mu_3\text{-}CNC_5H_4CH{=}CHC_6H_4OMe)]$ (**12**) showing the atom-numbering scheme.

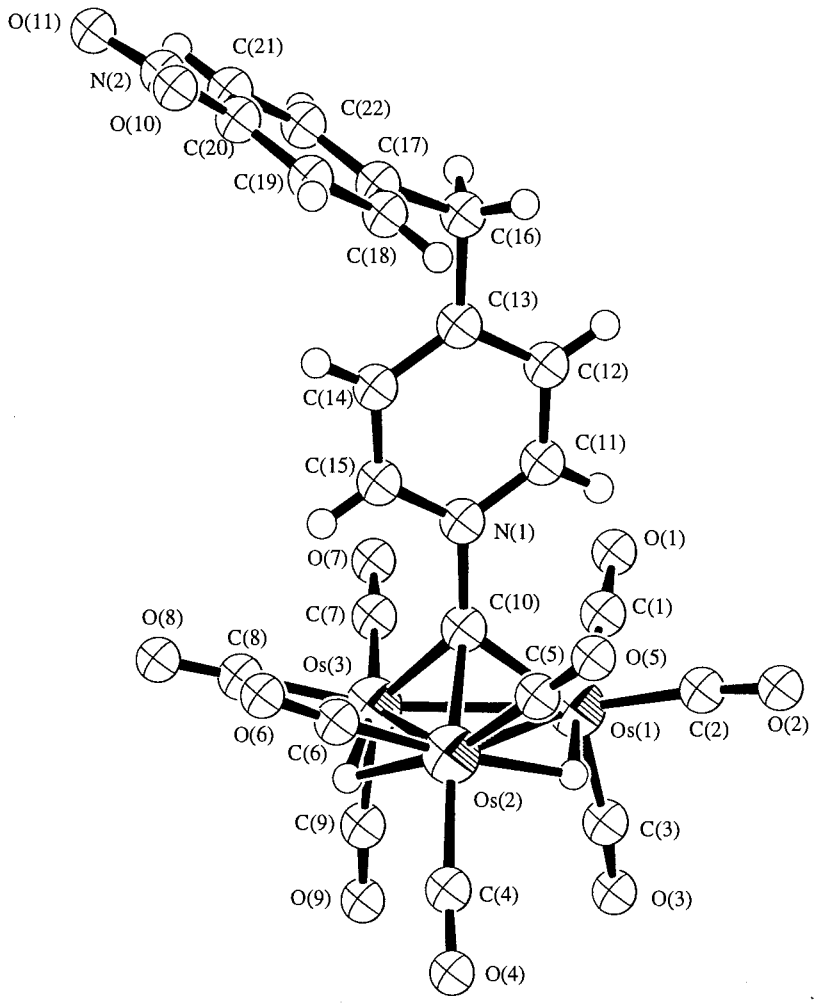

Fig. 5. Molecular structure of $[Os_3(\mu\text{-}H)_2(CO)_9(\mu_3\text{-}CNC_5H_4CH_2C_6H_4NO_2)]$ (**13**) showing the atom-numbering scheme.

instrument by either the electron impact (EI) or fast atom bombardment (FAB) technique. Electronic absorption spectra were obtained with a Perkin–Elmer Lambda UV–vis spectrophotometer. Preparative TLC was performed in air on 1 mm Kieselgel 60 silica plates.

4.2. Ligand syntheses

4.2.1. Schiff base ligands $NC_5H_4CH{=}NC_6H_4R$

A mixture of 4-pyridinecarboxaldehyde (0.03 mol) and the respective *para*-substituted aniline (0.03 mol)

Table 4
Selected bond distances (Å) and angles (°) for compound **7**

Bond distances (Å)					
Os(1)–Os(2)	2.8823(3)	Os(1)–Os(3)	2.7664(4)	Os(2)–Os(3)	2.8718(3)
Os(1)–C(10)	2.091(7)	Os(2)–C(10)	2.135(6)	Os(3)–C(10)	2.073(5)
N(1)–C(10)	1.446(8)	N(2)–C(16)	1.253(9)	N(2)–C(17)	1.40(1)
C(13)–C(16)	1.48(2)	Cl–C(20)	1.741(8)		
Bond angles (°)					
Os(2)–Os(1)–Os(3)	61.071(9)	Os(1)–Os(2)–Os(3)	57.472(8)		
Os(1)–Os(3)–Os(2)	61.457(9)	Os(1)–C(10)–N(1)	131.8(4)		
Os(2)–C(10)–N(1)	120.9(5)	Os(3)–C(10)–N(1)	133.1(5)		
N(2)–C(16)–C(13)	119.1(9)	C(16)–N(2)–C(17)	121.2(8)		
Cl–C(20)–C(19)	119.2(8)	Cl–C(20)–C(21)	119.5(6)		

in absolute ethanol or chloroform (30 cm^3) as solvent was heated to reflux and stirred for 2 h. The Schiff bases that separated on cooling were filtered off and washed with cold ethanol. The crude products were purified by repeated recrystallization from ethanol or chloroform, with yields of 70–80%. All components of the series were satisfactorily characterized by IR, ^{1}H-NMR and EI MS techniques.

R = H: m.p. 68–69°C; IR (Nujol, $\nu_{CH=N}$) 1621 cm^{-1}; ^{1}H-NMR ($CDCl_3$, J in Hz) δ 7.32 (m, C_6H_5), 7.75 (d, $J_{ab} = 6.1$, H_b), 8.45 (s, CH=N), 8.75 (d, $J_{ab} = 6.1$, H_a); M^+ (m/z) 182.

R = NMe_2: m.p. 197–198°C; IR (Nujol, $\nu_{CH=N}$) 1617 cm^{-1}; ^{1}H-NMR ($CDCl_3$, J in Hz) δ 2.98 (s, NMe_2), 6.72 (d, $J_{cd} = 8.8$, H_d), 7.32 (d, $J_{cd} = 8.8$, H_c), 7.70 (d, $J_{ab} = 6.1$, H_b), 8.46 (s, CH=N), 8.67 (d, $J_{ab} = 6.1$, H_a); M^+ (m/z) 225.

R = SMe: m.p. 82–83°C; IR (Nujol, $\nu_{CH=N}$) 1622 cm^{-1}; ^{1}H-NMR ($CDCl_3$, J in Hz) δ 2.52 (s, SMe), 7.24 (d, $J_{cd} = 8.8$, H_d), 7.29 (d, $J_{cd} = 8.8$, H_c), 7.75 (d, $J_{ab} = 6.1$, H_b), 8.47 (s, CH=N), 8.75 (d, $J_{ab} = 6.1$, H_a); M^+ (m/z) 228.

R = CMe_3: m.p. 65–66°C; IR (Nujol, $\nu_{CH=N}$) 1628 cm^{-1}; ^{1}H-NMR ($CDCl_3$, J in Hz) δ 1.35 (s, CMe_3), 7.21 (d, $J_{cd} = 8.8$, H_d), 7.46 (d, $J_{cd} = 8.8$, H_c), 7.75 (d, $J_{ab} = 6.1$, H_b), 8.48 (s, CH=N), 8.75 (d, $J_{ab} = 6.1$, H_a); M^+ (m/z) 238.

R = NH_2: m.p. 197–198°C; IR (Nujol, $\nu_{CH=N}$) 1617

Table 5
Selected bond distances (Å) and angles (°) for compound **8**

Bond distances (Å)					
Os(1)–Os(2)	2.880(1)	Os(1)–Os(3)	2.760(1)	Os(2)–Os(3)	2.868(2)
Os(1)–C(10)	2.07(2)	Os(2)–C(10)	2.11(2)	Os(3)–C(10)	2.08(2)
N(1)–C(10)	1.46(2)	N(2)–C(16)	1.25(3)	N(2)–C(17)	1.40(2)
C(13)–C(16)	1.46(3)	O(10)–C(20)	1.35(3)		
Bond angles (°)					
Os(2)–Os(1)–Os(3)	61.09(3)	Os(1)–Os(2)–Os(3)	57.39(3)		
Os(1)–Os(3)–Os(2)	61.52(3)	Os(1)–C(10)–N(1)	132(1)		
Os(2)–C(10)–N(1)	121(2)	Os(3)–C(10)–N(1)	132(2)		
N(2)–C(16)–C(13)	118(2)	C(16)–N(2)–C(17)	124(2)		
C(20)–O(10)–C(23)	121(3)				

Table 6
Selected bond distances (Å) and angles (°) for compound **12**

Bond distances (Å)					
Os(1)–Os(2)	2.8864(5)	Os(1)–Os(3)	2.8736(5)	Os(2)–Os(3)	2.7706(5)
Os(1)–C(10)	2.122(8)	Os(2)–C(10)	2.08(1)	Os(3)–C(10)	2.082(7)
N(1)–C(10)	1.47(2)	C(13)–C(16)	1.49(1)	C(16)–C(17)	1.32(1)
C(17)–C(18)	1.48(1)	O(10)–C(21)	1.39(1)		
Bond angles (°)					
Os(2)–Os(1)–Os(3)	57.51(1)	Os(1)–Os(2)–Os(3)	61.02(1)		
Os(1)–Os(3)–Os(2)	61.48(1)	Os(1)–C(10)–N(1)	120.9(5)		
Os(2)–C(10)–N(1)	132.2(5)	Os(3)–C(10)–N(1)	131.7(7)		
C(13)–C(16)–C(17)	123(2)	C(16)–C(17)–C(18)	127(1)		
C(21)–O(10)–C(24)	115(2)				

Table 7
Selected bond distances (Å) and angles (°) for compound **13**

Bond distances (Å)					
Os(1)–Os(2)	2.8796(9)	Os(1)–Os(3)	2.7579(9)	Os(2)–Os(3)	2.8620(8)
Os(1)–C(10)	2.08(1)	Os(2)–C(10)	2.10(1)	Os(3)–C(10)	2.06(1)
N(1)–C(10)	1.50(2)	N(2)–C(20)	1.56(3)	N(2)–O(10)	1.13(2)
N(2)–O(11)	1.19(2)	C(13)–C(16)	1.53(2)	C(16)–C(17)	1.56(2)
Bond angles (°)					
Os(2)–Os(1)–Os(3)	60.97(3)	Os(1)–Os(2)–Os(3)	57.42(2)		
Os(1)–Os(3)–Os(2)	61.61(3)	Os(1)–C(10)–N(1)	130(1)		
Os(2)–C(10)–N(1)	122.0(9)	Os(3)–C(10)–N(1)	133(1)		
C(13)–C(16)–C(17)	114(1)	O(10)–N(2)–C(20)	118(2)		
O(11)–N(2)–C(20)	115(2)	O(10)–N(2)–O(11)	128(3)		

cm^{-1}; ^{1}H-NMR ($CDCl_3$, J in Hz) δ 3.76 (br, NH_2), 6.72 (d, $J_{cd} = 8.8$, H_d), 7.22 (d, $J_{cd} = 8.8$, H_c), 7.72 (d, $J_{ab} = 6.1$, H_b), 8.48 (s, CH=N), 8.71 (d, $J_{ab} = 6.1$, H_a); M^+ (m/z) 197.

R = Cl: m.p. 82–83°C; IR (Nujol, $\nu_{CH=N}$) 1625 cm^{-1}; ^{1}H-NMR ($CDCl_3$, J in Hz) δ 7.16 (d, $J_{cd} = 8.8$, H_d), 7.37 (d, $J_{cd} = 8.8$, H_c), 7.71 (d, $J_{ab} = 6.1$, H_b), 8.40 (s, CH=N), 8.75 (d, $J_{ab} = 6.1$, H_a); M^+ (m/z) 216.

R = OMe: m.p. 95–96°C; IR (Nujol, $\nu_{CH=N}$) 1621 cm^{-1}; ^{1}H-NMR ($CDCl_3$, J in Hz) δ 3.80 (s, OMe), 6.92 (d, $J_{cd} = 8.8$, H_d), 7.27 (d, $J_{cd} = 8.8$, H_c), 7.70 (d, $J_{ab} = 5.9$, H_b), 8.42 (s, CH=N), 8.71 (d, $J_{ab} = 5.9$, H_a); M^+ (m/z) 212.

R = OC_6H_{13}: m.p. 58–59°C; IR (Nujol, $\nu_{CH=N}$) 1622 cm^{-1}; ^{1}H-NMR ($CDCl_3$, J in Hz) δ 0.91 (m, CH_3), 1.32–1.85 [m, $(CH_2)_4$], 3.98 (t, $J = 6.6$, OCH_2), 6.94 (d, $J_{cd} = 8.8$, H_d), 7.28 (d, $J_{cd} = 8.8$, H_c), 7.74 (d, $J_{ab} = 6.1$, H_b), 8.47 (s, CH=N), 8.73 (d, $J_{ab} = 6.1$, H_a); M^+ (m/z) 282.

R = OC_7H_{15}: m.p. 68–69°C; IR (Nujol, $\nu_{CH=N}$) 1621 cm^{-1}; ^{1}H-NMR ($CDCl_3$, J in Hz) δ 0.90 (m, CH_3), 1.32–1.85 [m, $(CH_2)_5$], 3.99 (t, $J = 6.6$, OCH_2), 6.94 (d, $J_{cd} = 8.8$, H_d), 7.29 (d, $J_{cd} = 8.8$, H_c), 7.74 (d, $J_{ab} = 5.9$, H_b), 8.48 (s, CH=N), 8.73 (d, $J_{ab} = 5.9$, H_a); M^+ (m/z) 296.

R = OC_9H_{19}: m.p. 70–71°C; IR (Nujol, $\nu_{CH=N}$) 1622 cm^{-1}; ^{1}H-NMR ($CDCl_3$, J in Hz) δ 0.89 (m, CH_3), 1.29–1.85 [m, $(CH_2)_7$], 3.99 (t, $J = 6.5$, OCH_2), 6.94 (d, $J_{cd} = 8.8$, H_d), 7.29 (d, $J_{cd} = 8.8$, H_c), 7.74 (d, $J_{ab} = 5.9$, H_b), 8.48 (s, CH=N), 8.73 (d, $J_{ab} = 5.9$, H_a); M^+ (m/z) 324.

4.2.2. Trans-stilbazole ligand $NC_5H_4CH{=}CHC_6H_4OMe$

To the commercially available 4-methoxybenzyltriphenylphosphonium chloride (2.0 g, 4.77 mmol), dissolved in dry benzene (50 cm^3), was added a 2.0 mol dm^{-3} hexane solution of *n*-butyllithium (2.4 cm^3, 4.80 mmol) at −78°C. The deep orange mixture was stirred under N_2 at −78°C for 0.5 h followed by the addition of 4-pyridinecarboxaldehyde (0.46 cm^3, 4.77 mmol). The reaction mixture which turned pale orange was then refluxed overnight. After filtering off most of the triphenylphosphine oxide, the solution was evaporated under reduced pressure to an oil. The oily residue was then purified by alumina chromatography using benzene as eluent to afford a mixture of the *trans*- and *cis*-isomers of 4′-methoxy-4-stilbazole. In this case, the pure *trans*-isomer was found to crystallize from the oil at −10°C and collected as a pale yellow solid in a 40% yield (0.40 g), leaving a yellow oil consisting mainly of the *cis*-isomer. M.p. 108–110°C; IR (KBr): 3075w, 3027w, 2963m, 2932m, 2878w, 2860w, 1734s, 1588vs, 1513vs, 1459s, 1416s, 1312s, 1284vs, 1261vs, 1215m, 1176vs 1123m, 1115m, 1073m, 1025vs, 971vs, 961s, 872m, 836vs; ^{1}H-NMR ($CDCl_3$): δ 8.52 (m, 2H, aromatic H), 6.77–7.54 (m, 6H, aromatic H), 3.84 (s, 3H, OMe); M^+ (m/z) 211.

*4.3. Synthesis of $[Os_3(\mu\text{-}H)_2(CO)_9(\mu_3\text{-}CY)]$ ($Y = NC_5H_4CH{=}NC_6H_4R$ (**1**–**11**), $NC_5H_4CH{=}CHC_6H_4OMe$ (**12**) and $NC_5H_4CH_2C_6H_4NO_2$ (**13**))*

The compound $[Os_3(\mu\text{-}H)_3(CO)_9(\mu_3\text{-}CCl)]$ (87.3 mg, 0.10 mmol) and each appropriate pyridine derivative (ten equivalents) were dissolved in CH_2Cl_2 (15 cm^3) and a DBU-CH_2Cl_2 solution (0.10 mmol) was added dropwise. The reaction mixture was stirred at r.t. for 30 min and subsequently concentrated under reduced pressure. In each case, purification was accomplished by TLC using *n*-hexane/CH_2Cl_2 (60:40, v/v) as eluent to yield the title complexes as a reddish–brown (for **1**–**11**), a bright red (for **12**) or an orange crystalline (for **13**) solid. The corresponding yields and R_f values are given as follows: **1**: $R_f = 0.6$, yield 39%; **2**: $R_f = 0.5$, yield 43%; **3**: $R_f = 0.6$, yield 41%; **4**: $R_f = 0.5$, yield 35%; **5**: $R_f = 0.4$, yield 34%; **6**: $R_f = 0.6$, yield 40%; **7**: $R_f = 0.6$, yield 50%; **8**: $R_f = 0.6$, yield 48%; **9**: $R_f = 0.7$, yield 38%; **10**: $R_f = 0.6$, yield 37%; **11**: $R_f = 0.5$, yield 35%; **12**: $R_f = 0.6$, yield 35%; **13**: $R_f = 0.5$, yield 38%.

5. Crystallography

Single crystals of suitable size and shape were chosen and mounted on glass fibre with epoxy resin under an optical microscope. Geometric and intensity data for **7**, **8**, **12** and **13** were collected on an Enraf–Nonius CAD4 diffractometer with graphite-monochromated Mo–K_α radiation ($\lambda = 0.71073$ Å) using the $\omega - 2\theta$ scan technique. The unit cell parameters of the compounds were determined by a least-square analysis of 25 accurately centred reflections. Data were collected at 298 K in the range $2 \leq 2\theta \leq 45°$. All pertinent crystallographic data are gathered in Table 8. The stability of the crystals was monitored at regular intervals using three standard reflections and no significant variation was observed. Intensity data were corrected for Lorentz and polarization effects and semi-empirical absorption corrections by the ψ-scan method were also applied. Scattering factors were taken from references [11a] and anomalous dispersion effects [11b] were included in F_c.

The structures were solved by a combination of direct methods (MULTAN 82) [12] and Fourier difference techniques. Refinements of structure were done on F by full-matrix least-squares analysis with all osmium and chlorine atoms refined anisotropically until convergence was reached. The hydrogen atoms of the organic moieties were generated in their ideal positions (C–H, 0.95 Å), while all metal hydrides were estimated by potential-energy calculations [7]. All hydrogens were included in structure factor calculations but not refined. Calculations were performed on a MicroVax II computer using the SDP package [13].

Table 8
Crystal data and data collection parameters for **7**, **8**, **12** and **13**

	7	**8**	**12**	**13**
Empirical formula	$C_{22}H_{11}N_2ClO_9Os_3$	$C_{23}H_{14}N_2O_{10}Os_3$	$C_{24}H_{15}NO_{10}Os_3$	$C_{22}H_{12}N_2O_{11}Os_3$
Molecular weight	1053.1	1048.6	1047.6	1050.6
Crystal size (mm)	$0.32\times0.32\times0.40$	$0.22\times0.24\times0.28$	$0.18\times0.26\times0.38$	$0.20\times0.21\times0.32$
Crystal system	Triclinic	Triclinic	Triclinic	Monoclinic
Space group	$P\bar{1}$	$P\bar{1}$	$P\bar{1}$	$P2_1/c$
a (Å)	8.199(1)	8.224(1)	8.344(1)	8.280(1)
b (Å)	12.505(2)	12.825(2)	12.384(2)	21.080(4)
c (Å)	13.917(2)	13.801(2)	14.055(3)	14.828(2)
α (°)	66.58(2)	66.23(2)	69.32(2)	90.0
β (°)	80.29(2)	79.98(2)	85.14(2)	95.45(2)
γ (°)	85.16(2)	84.38(2)	85.54(2)	90.0
U (Å^3)	1290.3(4)	1311.2(4)	1352.0(5)	2576.4(6)
$D_{calc.}$ (g cm^{-3})	2.710	2.656	2.573	2.708
Absorption coefficient (cm^{-1})	149.14	145.78	141.37	148.42
Z	2	2	2	4
$F(000)$	948	948	948	1896
2θ range (°)	2.0–45.0	2.0–45.0	2.0–45.0	2.0–45.0
Scan type	$\omega-2\theta$	$\omega-2\theta$	$\omega-2\theta$	$\omega-2\theta$
Scan speed (deg min^{-1} (in ω))	1.08–16.48	1.08–16.48	1.08–16.48	1.08–8.24
Scan range (ω deg^{-1})	$0.65+0.35\tan\theta$	$0.55+0.35\tan\theta$	$0.80+0.35\tan\theta$	$0.65+0.35\tan\theta$
Reflections collected	5426	4839	5095	3750
Independent reflections	5054	4604	4737	3475
Observed reflections [$F_o>3\sigma(F_o)$]	4343	3644	4181	2433
No. of parameters	334	342	168	168
Weighting scheme $w=4F_o^2/[\sigma^2(F_o^2)+p(F_o^2)^2]$	$p=0.05$	$p=0.04$	$p=0.04$	$p=0.04$
R, R_w	0.031, 0.040	0.062, 0.081	0.039, 0.055	0.037, 0.047
Goodness-of-fit	1.177	2.391	1.791	1.225
Residual extrema in final difference map (e Å^{-3})	1.241 to −1.783	2.731 to −2.413	1.244 to −1.661	1.175 to −0.896

6. Supplementary material

Crystallographic data (comprising hydrogen atom coordinates, thermal parameters and full tables of bond lengths and angles) for the structural analysis has been deposited with the Cambridge Crystallographic Centre (Deposition Nos. 114435 to 114438). Copies of this information may be obtained free of charge from The Director, CCDC, 12 Union Road, Cambridge, CB2 1EZ, UK (Fax: +44-1223-336-033; e-mail: deposit@ccdc.cam.ac.uk or www: http://www.ccdc.cam.ac.uk).

Acknowledgements

We acknowledge The Hong Kong Baptist University (W.-Y. Wong) and The University of Hong Kong (W.-T. Wong) for financial support.

References

[1] (a) M.A. Esteruelas, E. Sola, L.A. Oro, M.B. Ros, M. Macros, J.L. Serrano, J. Organomet. Chem. 387 (1990) 103. (b) M.A. Esteruelas, L.A. Oro, E. Sola, M.B. Ros, J.L. Serrano, J. Chem. Soc. Chem. Commun. (1989) 55. (c) C. Bertram, D.W. Bruce, D.A. Dunmur, S.E. Hunt, P.M. Maitlis, M. McCann, J. Chem. Soc. Chem. Commun. (1991) 69. (d) J.P. Rourke, F.P. Fanizzi, N.J.S. Salt, D.W. Bruce, D.A. Dunmur, P.M. Maitlis, J. Chem. Soc. Chem. Commun. (1990) 229. (e) W.-Y. Wong, W.-T. Wong, K.-K. Cheung, J. Chem. Soc. Dalton Trans. (1995) 1379. (f) W.-Y. Wong, S. Chan, W.-T. Wong, J. Chem. Soc. Dalton Trans. (1996) 2293.

[2] (a) W.T. Wong, J. Chem. Soc. Dalton Trans. (1998) 1253 and references cited therein. (b) W.-T. Wong, W.-Y. Wong, Acta Crystallogr. C51 (1995) 57.

[3] For example, see (a) W.-Y. Wong, S. Chan, W.-T. Wong, J. Organomet. Chem. 493 (1995) 229. (b) W.-Y. Wong, W.-T. Wong, J. Chem. Soc. Dalton Trans. (1995) 2831. (c) W.-Y. Wong, W.-T. Wong, J. Chem. Soc. Dalton Trans. (1996) 1853.

[4] M. Marcos, M.B. Ros, J.L. Serrano, M.A. Esteruelas, E. Sola, L.A. Sola, L.A. Oro, J. Barbera, Chem. Mater. 2 (1990) 748.

[5] Y. Iseki, E. Watanabe, A. Mori, S. Inoue, J. Am. Chem. Soc. 115 (1993) 7313.

[6] (a) B.F.G. Johnson, F.J. Lahoz, J. Lewis, N.D. Prior, P.R. Raithby, W.-T. Wong, J. Chem. Soc. Dalton Trans. (1992) 1701. (b) S. Chan, W.-Y. Wong, W.-T. Wong, J. Organomet. Chem. 474 (1994) C30.

[7] A.G. Orpen, J. Chem. Soc. Dalton Trans. (1980) 2509.

[8] A.P. Humphries, H.D. Kaesz, Prog. Inorg. Chem. 2 (1979) 145.

[9] W.L.F. Armarego, D.D. Perrin, Purification of Laboratory Chemicals, 4th edn, Butterworth–Heinemann, Guildford, UK, 1996.

[10] J.B. Keister, T.L. Horling, Inorg. Chem. 19 (1980) 2304.
[11] D.T. Cromer, J.T. Waber, International Tables for X-Ray Crystallography, vol. 4, Kynoch Press, Birmingham, 1974, (a) Table 2.2B; (b) Table 2.3.1.
[12] P. Mains, S.J. Fiske, S.E. Hull, L. Lessinger, G. Germain, J.P. Declercq, M.M. Woolfson, MULTAN 82, A System of Computer Programs for the Automatic Solution of Crystal Structures, Universities of York and Louvain, 1991.
[13] SDP Structure Determination Package, Enraf–Nonius, Delft, 1985.